2 Electromagnetic Wave Interactions with Water and Aqueous Solutions

Udo Kaatze

Drittes Physikalisches Institut, Bürgerstr. 42-44; D-37073 Göttingen; Germany

2.1 Introduction: Water, the Omnipresent Liquid

Water is the elixir of life on our planet. Molecular processes in the biosphere proceed almost exclusively in aqueous reaction media. The fact that water was present long before the evolution of life on earth suggests that its unique properties have strongly conditioned life as we know it. The water content of an adult human is as high as 65–70%. Generally, the content of water in living organisms ranges from about 96% in some marine invertebrates to somewhat less than 50% in bacterial spores [1]. Water does not just serve as a filling material in biological systems. It promotes the formation of biological structures, enables biological hydrolysis, and acts as a solvent distributing nutrients and removing metabolism products. The multiple functions of water in living organisms is also established by their inability to survive without a minimum supply of water. It is well known, for example, that dehydration of DNA leads to denaturation of this biopolymer.

Due to the ubiquity of water in our environment, this extraordinary chemical plays a key role in a variety of further aspects of human beings. About 95% of water available on our planet is contained in the large oceans, holding $1.3 \cdot 10^{21}$l. The Antarctic ice cap amounts to about 5% of this volume, namely $2.7 \cdot 10^{19}$l. The process of hydrological cycle mainly consists of evaporation from the oceans, subsequent precipitation and drain off back into the oceans. Within this cycle, around $1.3 \cdot 10^{16}$l of water are contained in the lower 11 kilometers of the atmosphere. The annual turnover of water amounts to $3.5 \cdot 10^{17}$l [1], leading to a continuous exposure of geological structures to water. The climate is evidently controlled by the humidity of the air but also by the moisture content of the soil. Consequences for agriculture are obvious.

In addition to the prominent role which water plays in ecological processes, it has many influences on sociological and industrial developments as well. Much industrial production would be impossible without water, like broad fields in chemical technology, power plant operation, flotation and dyeing in textile chemistry. A multitude of other areas of production and of maintenance of products depends sensitively on the water content of material. Examples are efficient oil recovery, the strength of bricks, the consistency of cosmetics, and the storage life of food-

stuff. There are thus many reasons for a better understanding of the eccentric properties of water. In view of the widespread and still increasing use of electromagnetic waves, there are particular demands for deeper insights into their interactions with this omnipresent chemical. A brief tutorial on some aspects of electromagnetic wave interactions with aqueous systems is given. Details and references to original articles are presented in recent reviews on the dielectric properties of water [2–5] and aqueous solutions [6–10].

2.2 The Architecture of the Water Molecule and the Unique Hydrogen Network

2.2.1 The Isolated Water Molecule

The unusual properties of water and its multiple functions in the biosphere and in technology are related to the architecture of the H_2O molecule. As sketched in Fig. 2.1, the water molecule can be roughly represented by a regular tetrahedron with an oxygen atom at its center, with two protons at two of its vertices, and with lone pair electrons in orbitals directed toward both other vertices. The H–O–H angle is somewhat smaller than the angle 109.5° of a tetrahedron. Values in the literature vary between 104.45° and 105.05°. The electrical charges are not uniformly distributed over the water molecule so that the vertices of the tetrahedron constitute poles of electrical charges, of which two are positive since the hydrogen nuclei are not completely screened by the binding electrons. The lone pair of electrons at the other two vertices hold the corresponding negative charges. These charges amount to about $0.17e$ and $-0.17e$, respectively, where $e = 1.602 \cdot 10^{-19}$ As denotes the elementary charge [4, 5].

Because of the particular charge distribution, the water molecule, besides its electrical polarizability $\alpha = 1.444 \cdot 10^{-30} m^3$ due to electronic and atomic displacement polarizabilities, possesses also a permanent electric dipole moment, $\mu = (1.84 \pm 0.02)$ D, resulting from the vector sum of the two H–O bond moments of 1.53D. Here 1D, the commonly used unit of the molecular electric dipole moment, corresponds with 10^{-18}esu $= 1/3 \cdot 10^{-29}$As.

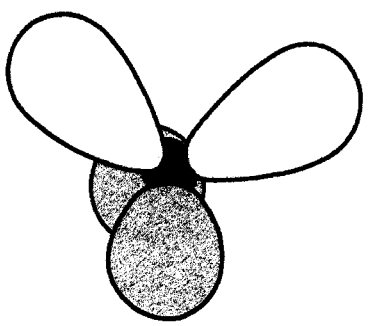

Fig. 2.1. Sketch of a water molecule as a regular tetrahedron [5]. The oxygen is shown in black. Light and dark areas show the binding orbitals to the hydrogen molecules and the lone electron pairs, respectively

The water molecule also possesses quadruple moment components. The mean quadruple moment almost vanishes. Hence it is the permanent electric dipole moment that mediates electromagnetic wave interactions with water molecules.

2.2.2 Liquid Water

Because of the positive electrical charges at the only partially shielded protons and the negative electrical charges of the lone electron pairs, water molecules interact to form hydrogen bonds. As illustrated by Fig. 2.2, the binding hydrogen atom in a water dimer forms a covalent bond to one oxygen and a hydrogen bond to the oxygen of the other water molecule. The bond strength differs by an order of magnitude. The enthalpy of the covalent H–O bond is as high as 463 kJ/mol, whereas that of the hydrogen bond is about 20 kJ/mol only. The most stable configuration of a hydrogen bond is a linear H–O-H arrangement. In ice, the distance between two hydrogen bonded oxygens is 0.276 nm with the hydrogen being 0.101 nm apart from one oxygen atom and 0.175 nm from the other one. The H-bond is largely ionic in character, with covalent parts that can be neglected on many events [4, 5].

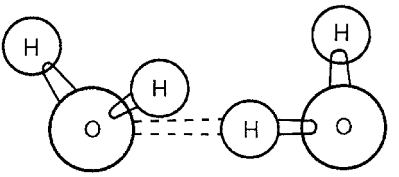

Fig. 2.2. Hydrogen bonded linear water dimer

As each water molecule is capable of four hydrogen bonds, a macroscopically percolating three-dimensional H-bonded network is formed in the condensed phases. For hexagonal ice, the ordered hydrogen network structure is illustrated by Fig. 2.3. Computer simulation studies of liquid water reveal the bond order j_b ($j_b = 0...4$) to follow a binominal distribution. Hence j_b may be considered a random quantity. Water molecules bound by more than one H-bond are prevented from reorientational motions. Consequently, only the molecules which, at a time, are non- or single-hydrogen bonded ($j_b = 0,1$) are able to rotate the direction of their permanent electric dipole moment into the direction of an external electric field and thus to contribute to the orientational polarization.

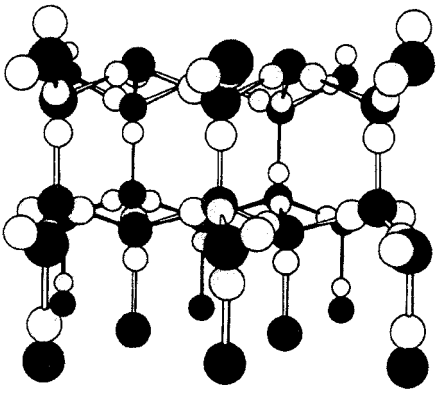

Fig. 2.3. Hexagonal structure of ice-Ih

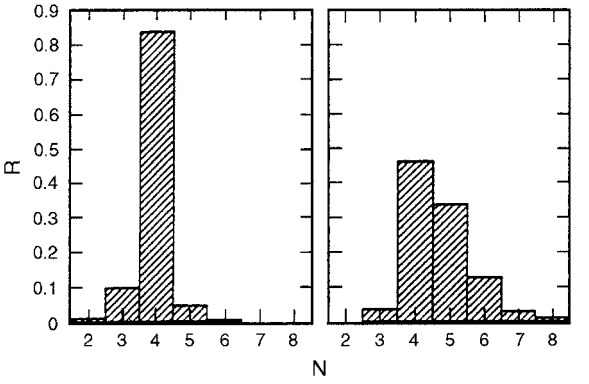

Fig. 2.4. Fraction R of molecules with N neighbors within a distance of 0.33 nm for water at 0°C and at reduced (left side, $\rho = 0.75$ g cm^{-3}) as well as normal (right side, $\rho = 1$ g cm^{-3}) pressure [4]

Computer simulations also show that, at reduced density ρ, almost perfect tetrahedral order is adopted in water. The fraction R_4 of molecules with four neighbors within a distance $r = 0.33$ nm in water at 0°C amounts to more than 80 per cent at $\rho = 0.75$g cm^{-3}. On normal conditions ($\rho = 1$g cm^{-3}) less than 50 per cent of the water molecules are fourfold coordinated and about one-third of all molecules reveals five neighbors within the $r = 0.33$ nm distance (Fig. 2.4). Hence the regular tetrahedral structure of ice, yielding a tridymite-like lattice in which the oxygen atoms form puckered six-membered rings (Fig. 2.3), is significantly disturbed in water on normal conditions. The defects in the water structure resulting thereby lead to far reaching consequences for the microdynamics of water. The much higher number of defects, for example, is the reason why the dielectric relaxation time of liquid water at 0°C ($\tau = 17.7$ps) is by six orders of magnitude smaller than the relaxation time of ice ($\tau = 20\mu$s) at the same temperature.

The fact that, within the hydrogen bond network of water, the energy of the covalent bond exceeds that of the hydrogen bond by a factor of more than twenty suggests the idea of well-defined water molecules also for the condensed phases. There exists nevertheless an autoprotolysis equilibrium $2H_20 \Leftrightarrow 0H^- + H_30^+$ in the liquid, with considerable import for chemistry and biology. The equilibrium constant of the autoprotolysis, however, is small ($pK_w = 14$, 25°C) so that there is only a small ion concentration in pure water.

2.3 Hydrogen Network Fluctuations and Polarization Noise

Since the enthalpy of a hydrogen bond (20 kJ/mol) is on the order of the thermal energy at room temperature (RT = 2.5 kJ/mol, 25°C) the bond strength of the hydrogen network of water fluctuates rapidly due to thermal agitation. Fluctuation correlation times as small as 0.1 to 1 ps have been reported. Normally, after the weakening of a bond, however, the same bond is reformed again. Reorientation of a water molecule through a significant angle and thus formation of a hydrogen bond at another site occurs only on favorable conditions. These conditions include the existence of an additional neighbor, the "fifth neighbor", in a suitable position. Such a neighbor constitutes a network defect with considerable importance to the reorientational motions of water. The additional neighbor molecule promotes the formation of a branched (bifurcated) hydrogen bond and flattens the potential energy barriers between different network fluctuations. Reorientational motions are significantly facilitated thereby, particularly as the additional neighbor offers a site for the formation of a new bond. For water at room temperature, it takes about 10 ps until a fifth neighbor molecule is present in a position that promotes reorientation. The reorientation of a molecule itself into a new direction resembles a switching process since it occurs again in a short period of about 0.1 ps. Hence the reorientational motions of water molecules in the liquid may be characterized by a wait-and-switch process in which the reorientation time is predominantly governed by the period for which a water molecule has to wait until favorable conditions for the reorientation exist. As it is essential for these conditions that an additional hydrogen bonding neighbor has to approach, the orientational motions of the water molecules are evidently controlled by the concentration of partners capable of forming H-bonds. The higher this concentration, the larger the probability for the availability of the additional neighbor – hence the smaller the reorientation time of the water molecules [5, 10].

Since the water molecules are provided with a permanent electric dipole moment, their reorientational motions will produce electrical polarization noise. In principle, this noise could be used to measure the dielectric properties of the aqueous systems under study, in particular to determine the time constants of interest. Let us, for simplicity, consider an imaginary experiment. The dipolar liquid may be contained in an ideal plane parallel-plate capacitor with the distance between the plates small as compared to their lateral dimensions. To be able to monitor all changes in the

electrical charges on the plates, the capacitor is connected to a suitable instrument with vanishing internal impedance.

Thermal fluctuations in the electrical polarization $\vec{P}$ of the dipolar liquid induce electrical charges on the plates of the capacitor. For isotropic liquids the amount of charges is proportional to the amount $P = |\vec{P}|$ of the dielectric polarization. The noise signal monitored by this experiment (Fig. 2.5) displays two essentially different molecular processes. Fast changes in the signal result from electronic and atomic displacement polarization mechanisms, slower variations in the noise are due to the reorientational motions of the dipolar molecules. The details in the time-dependent properties of the noise are reflected in an obvious manner by the normalized auto-correlation function [5, 7]

$$\phi(t) = < P(t) \cdot P(0) > / < P(0) \cdot P(0) > \tag{2.1}$$

also named "dielectric decay function". For water at 25°C, as an example, the autocorrelation function of the polarization noise is shown in Fig. 2.5. Due to the fast displacement polarization mechanisms and also to a high frequency relaxation process, the decay function decreases rapidly from $\phi = 1$ at $t = 0$ to $\phi(t_0) = 0.94 \cdot \phi(0)$ at $t = t_0$. The slower decay in the autocorrelation function represents the reorientational motions of the water molecules. This part of the autocorrelation function at $t > t_0 = 2 \cdot 10^{-12}$s (=2 ps) follows almost an exponential

$$\phi(t > t_0) = \phi(t_0) \exp(-(t - t_0) / \tau_w) \tag{2.2}$$

The decay time τ_w will be named principal dielectric relaxation time of water in the following. As mentioned above, for water at room temperature τ_w is on the order of 10 ps. Notice, that the dielectric relaxation time of water corresponds with the macroscopic polarization.

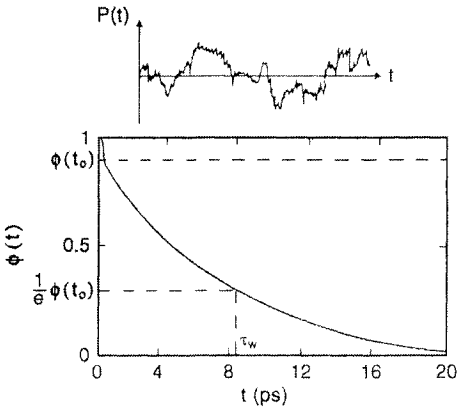

Fig. 2.5. Polarization noise (top) and autocorrelation function $\phi(t)$ (Eq. (2.1)) for water at 25°C (bottom)

Hence it is not the reorientation time of individual water molecules but rather a collective quantity. It is a measure of the period over which, at thermal equilibrium, the direction of the polarization is correlated to an originally existing direction.

2.4 The Dielectric Properties of Water

2.4.1 Complex Permittivity Spectrum

Due to the unavoidably existing noise of the measurement system itself, analysis of the noise signal of real experiments is difficult. For this reason, it is more convenient to expose the sample liquid to a disturbing electromagnetic signal. In doing so the field strength of the signal has to be sufficiently small to guarantee the sample remains in almost thermal equilibrium and thus avoid any nonlinear effects during the measurements. The advantage taken from the use of an external signal is the small preferential orientation of all dipolar molecules that is superposed to the thermally driven reorientational motions, resulting in a substantial enhancement of the signal-to-noise ratio. Two different types of disturbances are common in measurements of the principal dielectric relaxation of water. Sequences of step-voltage pulses are used in time domain spectrometry (TDS) that probes the dielectric decay function $\phi(t)$. Alternatively, sinusoidally varying electromagnetic fields $E(\nu)$ are applied in frequency domain techniques. The electric polarization $P(\nu)$ is then not only a function of the electric field strength E but also of the frequency ν. Since, due to molecular interactions, the polarization needs a finite time to establish, it cannot follow electrical field changes instantaneously. Hence there exists a dispersion in $P(\nu)$. In addition, a phase shift between $P(\nu)$ and $E(\nu)$ occurs in the dispersion region. Energy of the external electromagnetic field is dissipated as heat. Both effects, the dispersion in the polarization and the absorption of electromagnetic energy, are considered by a frequency dependent complex permittivity [5–7]

$$\varepsilon(\nu) = \varepsilon'(\nu) - i\varepsilon''(\nu) = \frac{P(\nu)}{\varepsilon_0 E(\nu)} + 1 \tag{2.3}$$

Here, ε_o denotes the electric field constant and $i^2 = -1$. According to linear system theory the transfer function $\varepsilon(\nu)$ and the step response function $\phi(t)$ are related as

$$\varepsilon(\nu) = (\varepsilon(0) - 1) \int_o^\infty \left[-\frac{d\phi(t)}{dt} \right] e^{-i2\pi\nu t} dt + 1 \tag{2.4}$$

where $\varepsilon(0) = \lim_{\nu \to 0} \varepsilon'(\nu)$ is the low frequency ("static") permittivity of the dielectric.

As $\phi(t)$ is a real function the real part $\varepsilon'(\nu)$ and the negative imaginary part $\varepsilon''(\nu)$ of the complex permittivity are not independent from one another but are different forms of the same phenomena, the relaxation of the dielectric.

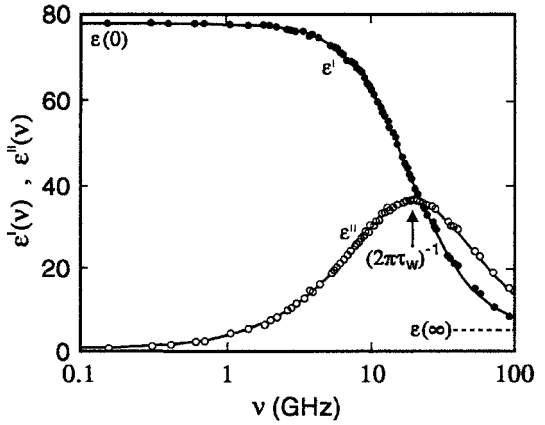

Fig. 2.6. Real part ε' and negative imaginary part ε'' of the complex permittivity spectrum of water at 25°C. Microwave permittivity data have been taken from the literature [2, 3]. Lines are graphs of Eq. (2.5) with parameter values of Table 2.1

Table 2.1. Dielectric parameters of water at different temperatures T: Static permittivity values as recommended by the IUPAC Commission on Physico-Chemical Measurements and Standards [14] and parameters of Eq. (2.5) as following from a regression analysis of microwave complex permittivity data ($\nu < 100$ GHz, [2, 5])

T/°C	$\varepsilon(0)$, [14]	$\varepsilon(0)$	$\varepsilon(\infty)$	τ_w, ps
0	87.87 ± 0.07	87.91 ± 0.2	5.7 ± 0.2	17.67 ± 0.1
0.3		87.70 ± 0.2	5.9 ± 0.2	16.42 ± 0.2
5		85.83 ± 0.2	5.8 ± 0.2	14.50 ± 0.4
10	83.91 ± 0.07	83.92 ± 0.2	5.8 ± 0.3	12.68 ± 0.1
15		82.05 ± 0.2	6.0 ± 0.2	10.84 ± 0.1
20	80.16 ± 0.05	80.21± 0.2	5.7 ± 0.2	9.37 ± 0.05
25	78.36 ± 0.05	78.36 ± 0.05	5.4 ± 0.2	8.28 ± 0.02
30	76.57 ± 0.05	76.56 ± 0.2	5.2 ± 0.3	7.31 ± 0.05
35		74.87 ± 0.2	5.3 ± 0.4	6.54 ± 0.1
37		74.17 ± 0.2	5.3 ± 0.2	6.27 ± 0.1
40	73.16 ± 0.04	73.18 ± 0.2	4.6 ± 0.7	5.82 ± 0.1
50	69.90 ± 0.04	69.89 ± 0.2	4.0 ± 0.5	4.75 ± 0.1
60	66.79 ± 0.04	66.70 ± 0.2	4.2 ± 0.5	4.01 ± 0.1
70	62.82 ± 0.05			
80	61.03 ± 0.05			
90	58.32 ± 0.05			
100	55.72 ± 0.06			

The exponential dielectric decay function (Eq. (2.2)) corresponds with a Debye-type relaxation spectral function, defined by the relation

$$\varepsilon(\nu) = \varepsilon(\infty) + \frac{\varepsilon(0) - \varepsilon(\infty)}{1 + i\omega\tau_w} \tag{2.5}$$

with $\omega = 2\pi\nu$ and $\varepsilon(\infty) = \lim_{\nu\to\infty} \varepsilon'(\nu)$ denoting the permittivity as extrapolated to frequencies well above the relaxation frequency ($\nu >> (2\pi\tau_w)^{-1}$). Parameter $\varepsilon(\infty)$ reflects the rapidly decaying polarization processes in $\phi(t)$, with relaxation times smaller than t_o (Fig. 2.5).

In the microwave region up to frequencies of about 100 GHz, the complex dielectric spectrum of water can be well represented by a Debye type relaxation function. As an example the permittivity spectrum at 25°C is shown in Fig. 2.6, where the meaning of the parameters of Eq. (2.5) is also indicated. It is only mentioned that another low amplitude relaxation term has been found toward higher frequencies, with relaxation time around 0.2 ps (19°C). Within the framework of the wait-and-switch model outlined above this relaxation term has been attributed to the single hydrogen bonded water molecules. The concentration of such molecules is small and thus the relaxation amplitude is also small. The content of molecules with more than one hydrogen bond, providing a suitable site to the single-hydrogen bonded water molecules for the formation of a new bond, is larger. Hence the time for which a molecule with only one H-bond has to wait until favorable conditions for reorientation occur is small and likewise small is the dielectric relaxation time [10].

Here the discussion will be restricted to the microwave region of the spectrum ($\nu \leq 100$ GHz). Hence $\varepsilon(\infty)$ means the high frequency limit of the dominating relaxation process with relaxation frequency $(2\pi\tau_w)^{-1}$ of about 20 GHz (25°C), Fig. 2.6). The parameters of the corresponding relaxation spectral function (Eq. (2.5)) are displayed in Table 2.1.

2.4.2 Static Permittivity

Due to the rather high permanent electric dipole moment $\mu = 1.84$D of the water molecule in the gaseous state, liquid water exhibits a large static permittivity. It decreases from $\varepsilon(0) = 107 \pm 2$ for supercooled water at –35°C to $\varepsilon(0) = 87.87 \pm 0.07$ at 0°C and finally to $55.62 \pm 0.02 \leq \varepsilon(0) \leq 55.72 \pm 0.06$ at 100°C and normal pressure [2, 3, 5]. Various empirical relations have been reported to analytically represent the temperature dependence of the static permittivity of water. In Fig. 2.7 a plot is given of the simple equation [7]

$$\varepsilon(0) = 87.853 \exp[-0.00457(T/\mathrm{K} - 273.15)] \tag{2.6}$$

to show that, in the temperature range between –25 and 100°C, it represents the experimental data within the limits of errors. Only for supercooled liquid water at even lower temperatures do the deviations between the measured data and the predictions from Eq. (2.6) somewhat exceed the experimental errors.

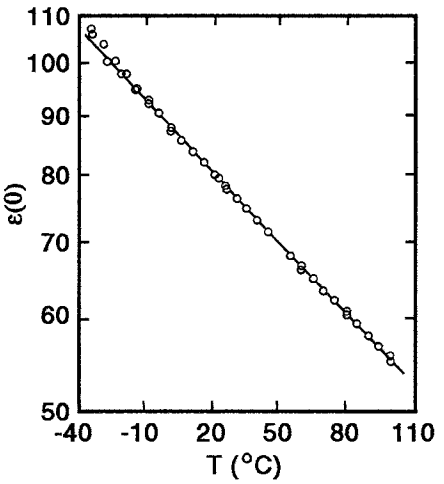

Fig. 2.7. Static permittivity $\varepsilon(0)$ of water on a logarithmic scale versus temperature T (Table 2.1). The line represents a simple empirical relation (Eq. (2.6))

Theoretical models relate to the static permittivity of a dipolar liquid to the dipole moment μ, to the dipole concentration c, and to the Kirkwood orientation correlation factor g [5, 7]

$$\frac{(\varepsilon(0)-\varepsilon_\infty)(2\varepsilon(0)+\varepsilon_\infty)}{\varepsilon(0)} = \frac{N_A}{9\varepsilon_0 k_B T}(\varepsilon_\infty+2)^2 c\mu g \qquad (2.7)$$

In this equation N_A denotes Avogadro's number and k_B the Boltzmann constant. The orientation correlation factor considers the fact that preferential parallel alignment of dipole moments results in an enhanced static permittivity ($g > 1$), as evident from the dielectric properties of ferroelectrics, and that antiparallel ordering of dipole moments leads to a reduction in the static permittivity ($g < 1$). For water the situation is less clear. The reason is our insufficient knowledge of the high frequency permittivity ε_∞ ($n^2 \le \varepsilon_\infty \le \varepsilon(\infty)$) to be used in Eq. (2.7). Here n is the optical refractive index. Kirkwood using $\varepsilon_\infty = n^2 = 1.33^2$ found $g = 2.8$ whereas $\varepsilon_\infty = \varepsilon(\infty)$ yields $g < 1$. It has been shown that $\varepsilon_\infty = 4.3$ is in conformity with $g = 1$, which would suggest effects of orientation correlation in liquid water to be absent at all. In this context, it is interesting to notice that the aforementioned high frequency relaxation term with relaxation time on the order of 0.2 ps (Fig. 2.8) extrapolates to $\varepsilon^*(\infty) = \lim_{\nu\to\infty}\varepsilon'(\nu) = 3.4$ at $\nu > (2\pi\tau_w^*)^{-1}$. Despite of the still insufficient knowledge about the effect of orientation correlation in the static permittivity of water, Eq. (2.7) indicates that reorientation of permanent dipole moments occurs against thermal agitation, tending at equipartition of all states of dipole orientation.

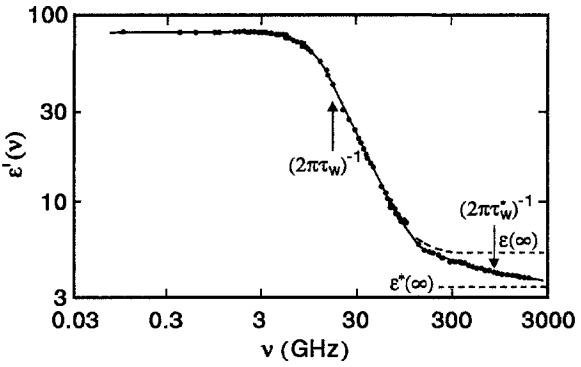

Fig. 2.8. Bilogarithmic plot of the real part of permittivity spectrum up to some THz of water at 19°C [10]

2.4.3 High Frequency Properties

In Fig. 2.9 the extrapolated high frequency permittivty $\varepsilon(\infty)$ as following from Eq. (2.5) is displayed as a function of temperature T. At low temperatures the experimental $\varepsilon(\infty)$ values significantly exceed the high frequency permittivity data that have been determined by assuming $g = 1$ and treating ε_∞ as an adjustable parameter in Eq. (2.7). At higher temperatures ($T \geq 50°C$), however, both sets of data almost agree with one another. Interesting, the $\varepsilon^*(\infty)$ data which, according to

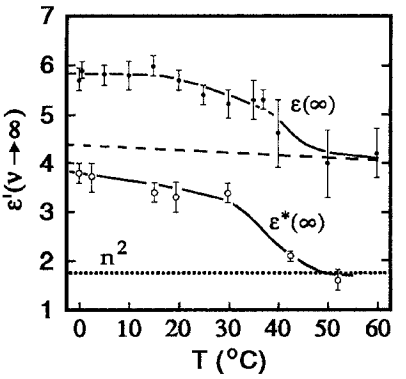

Fig. 2.9.
Extrapolated high frequency permittivities $\varepsilon(\infty)$ and $\varepsilon^*(\infty)$ (Fig. 2.8) and squared optical refractive index n^2 of water versus temperature T

$$\varepsilon(\nu) = \varepsilon^*(\infty) + \frac{\varepsilon(\infty) - \varepsilon^*(\infty)}{1 + i\omega\tau_w^*} + \frac{\varepsilon(0) - \varepsilon(\infty)}{1 + i\omega\tau_w} \tag{2.8}$$

have been determined from the spectra which include complex permittivities from THz measurements (Fig. 2.8), also decrease at temperatures higher than 30°C and reach the squared optical refraction index at $T = 50°C$. Hence $\varepsilon(\infty)$ seems to just follow the trend in $\varepsilon^*(\infty)$. The relative contribution $(\varepsilon(\infty)-\varepsilon^*(\infty))/(\varepsilon(0)-\varepsilon(\infty))$ of the fast relaxation process to the static permittivity of water increases from 0.025

at 0°C to 0.034 at 50°C. This finding may be taken to support the assignment of the fast relaxation term to the reorientational motions of single hydrogen bonded water molecules, because their concentration is expected to increase with T [10]. Also in conformity with the experimental facts, however, is the assumption of the high frequency relaxation to reflect the reorientation of non-hydrogen bonded interstitial water molecules.

2.4.4 Principal Relaxation Time

The wait-and-switch model of water reorientation outlined above implies a potential barrier between two orientations of a water dipole moment as sketched in Fig. 2.10. Normally a water molecule is contained in either of the potential minima where the strength of its hydrogen bonds fluctuates rapidly with correlation times on the order of 0.12 to 1 ps, as also mentioned above. Due to thermal activation, e.g. due to collision with neighboring water molecules, a water molecule will occasionally posses a kinetic energy that is higher than the potential barrier and will thus be able to surmount it and to orientate its dipole moment in another direction [4, 5, 7, 10]. The effect from the additional neighbor in the wait-and-switch model is a reduction of the potential energy separating different dipole orientations, as indicated by the dashed curve in Fig. 2.10.

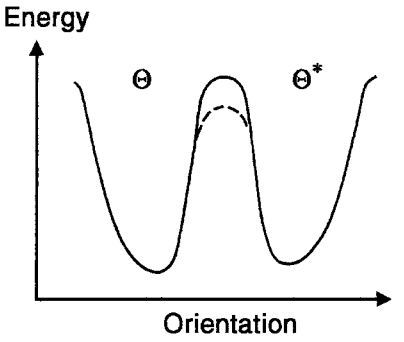

Fig. 2.10.
Sketch of a potential energy barrier separating two directions θ and θ^* of permanent dipole moment. The dashed line shows the reduction in the energy barrier due to a suitable additional neighbor molecule

Because of the idea of an underlying thermal activation mechanism, it is an obvious attempt to assume the dielectric relaxation time τ_w of the dominating relaxation term of water to be governed by a Gibbs free energy of activation

$$\Delta G^{\#} = \Delta G^{\#} - T\Delta S^{\#} \tag{2.9}$$

and thus to be given by an Eyring relation [6]

$$\tau_w = \frac{h}{k_B T} C \exp(\Delta G^{\#} / RT) \tag{2.10}$$

Here $\Delta H^{\#}$ and $\Delta S^{\#}$ are the activation enthalpy and entropy, respectively, h is Planck's constant, C a configurational factor, and $R = k_B N_A$ denotes the gas constant. From the $\ell n \tau_w$-vs-T^{-1} plot in Fig. 2.11 $\Delta H^{\#} = (16.7 \pm 0.4)$kJ/mol and $\Delta S^{\#} = (23 \pm 2)$ J/(mol K) follows. Hence the activation enthalpy is on the order of the interaction enthalpy $\Delta H = 20$ kJ/mol of hydrogen bonds in water.

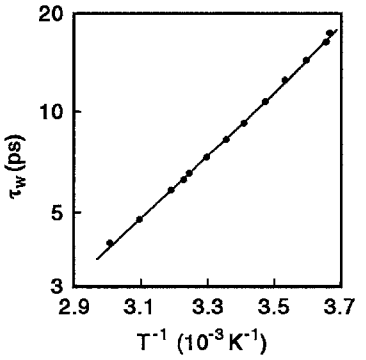

Fig. 2.11. Eyring plot of the relaxation time τ_w of water. Errors do not exceed the symbols

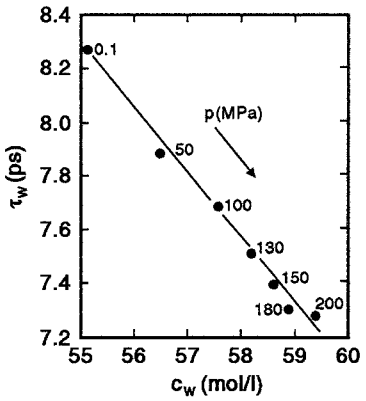

Fig. 2.12. Relaxation time τ_w of water as a function of water concentration [11]. Parameter is the hydrostatic pressure p

The quantities $\Delta H^{\#}$ and $\Delta S^{\#}$ refer to molecular rather than collective mechanisms and should thus be calculated from the dipole rotational relaxation times instead of the dielectric relaxation times τ_w. There exists, however, a nice correlation between the temperature dependencies of the proton magnetic relaxation rate $1/T_1$, reflecting the proton-around-proton reorientational motion of a water molecule, and τ_w. Therefore, the activation enthalpy from the dipole rotational correlation times almost agrees with that from the principal dielectric relaxation time τ_w.

It is well established that the principal dielectric relaxation time decreases when water is exposed to a hydrostatic pressure p. Due to the pressure the density of water increases and therefore increases the water concentration (Fig. 2.12). Hence the reduction of the dielectric relaxation time with p may be taken another confirmation of the wait-and-switch model of water reorientation.

2.5 Aqueous Solutions

2.5.1 Solute Contributions to Dielectric Spectra

In Fig. 2.13 the complex permittivity spectrum of a 1-molar aqueous solution of nondipolar quinoxaline is shown and compared to that of water at the same temperature. Due to the dilution of the dipolar water by the nonpolar solute the static permittivity of the solution is substantially smaller than that of the solvent. Additionally, because of the particular molecular interactions introduced by the solute molecules, the dispersion ($d\varepsilon'(\nu)/d\nu < 0$) and dielectric loss region extends over a broader frequency range than in water and is shifted to lower frequencies. These effects increase with solute concentration c [6, 7, 10]. The broadening of the relaxation region, which reflects a distribution of relaxation times, can be considered by a Havriliak–Negami relaxation spectral function [9]

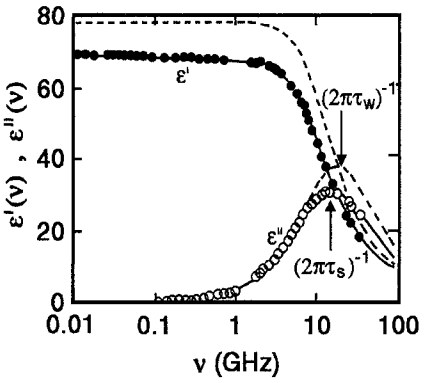

Fig. 2.13. Complex permittitivy spectrum for a 1 mol/ℓ aqueous solution of quinoxaline at 25°C [7, 9]. Dashed lines indicate the spectrum of water at the same temperature

$$\varepsilon(\nu) = \varepsilon(\infty) + \frac{\varepsilon(0) - \varepsilon(\infty)}{(1 + (i\omega\tau_s)^{1-h})^{1-b}} \tag{2.11}$$

Here, τ_s is a characteristic relaxation time of the underlying distribution function and parameters h and b control the shape and width of the relaxation time distribution. Eq. (2.11) includes some well-known and frequently used spectral functions, the Cole–Cole ($b = 0$), the Davidson–Cole ($h = 0$), and the Debye function ($b = h = 0$). With the notation $\tau_s = \tau_w$ the latter corresponds with Eq. (2.5).

A summary of results for aqueous solutions of low weight organic molecules is given in [7]. Also discussed in that article and especially in [8, 12] are spectra for aqueous solutions of low weight electrolytes and polyelectrolytes. As an example, the complex permittivity spectrum of a sodium chloride solution is shown in Fig. 2.14. The salt concentration corresponds with that of the North Sea. A particular feature of electrolyte solutions is the strong increase in the ε'' data towards low frequencies which results from the contribution of the ionic conductivity σ. With the conductivity term $-i\sigma/(\varepsilon_o\omega)$ the spectral function

$$\varepsilon(\nu) = \varepsilon(\infty) + \frac{\varepsilon(0) - \varepsilon(\infty)}{(1 + (i\omega\tau_s)^{1-h})^{1-b}} - \frac{i\sigma}{\varepsilon_0 \omega} \tag{2.12}$$

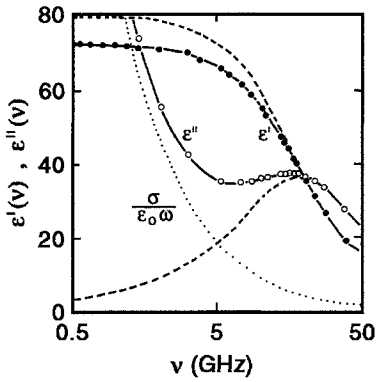

Fig. 2.14. Complex dielectric spectrum for a 0.61 mol/l aqueous solution of NaCl at 25°C [9]. The dotted curve shows the conductivity contribution to ε''. Dashed lines indicate the spectrum of water at 25°C

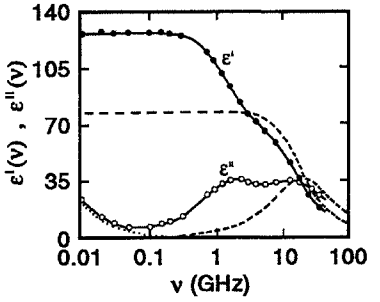

Fig. 2.15. Complex permittivity spectrum for a 1 mol/l solution of 4-aminobutyric acid in water at 25°C and at neutral pH [9]. Dashed lines represent the water spectrum at 25°C

results which at low frequencies is dominated by the σ contribution. Quite remarkably there is also a significant reduction in the static permittivity (Fig. 2.14) which, at least in parts, reflects the preferential orientation of the dipolar water molecules in the Coulombic field of small cations. This effect is normally named dielectric saturation or structure saturation.

Spectra for aqueous solutions of dipolar solutes often display two well-separated relaxation regions of which one is due to the water and the other one to the solute reorientational motions. An example is given in Fig. 2.15 for a solution of 4-aminobutyric acid in water. The large solute electric dipole moment of about 20D leads to a large amplitude in the corresponding (low frequency) relaxation term though the aminobutyric acid concentration is distinctly smaller than that of water. As not all solute molecules are zwitterionic, some ionic species contribute also a conductivity term to the spectrum. The complex permittivity may thus be analytically represented by the relaxation spectral function

$$\varepsilon(\nu) = \varepsilon(\infty) + \frac{\varepsilon(0) - \varepsilon(\infty)}{(1 + (i\omega\tau_s)^{1-h})^{1-b}} + \frac{\varepsilon(0)}{1 + i\omega\tau_0} - \frac{i\sigma}{\varepsilon_0 \omega} \tag{2.13}$$

where ε^* is the low frequency limit of the water dispersion as well as the high frequency limit of the solute dispersion. Parameter τ_u is the dielectric relaxation time of the solute.

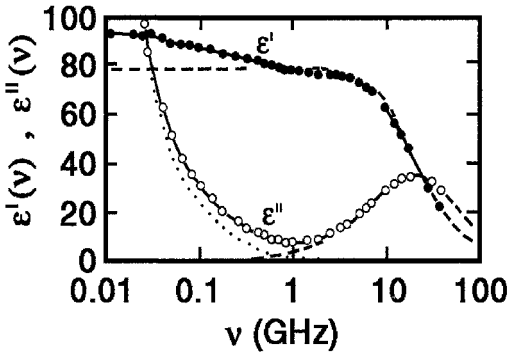

Fig. 2.16. Complex dielectric spectrum of a 0.06 mol/l aqueous solution of the cationic surfactant n-hexadecyltrimethylammonium bromide at 25°C [9]. The dotted curve shows the conductivity contribution to ε''. Dashed lines indicate the water spectrum at the same temperature

Solute contributions with relaxation characteristics may also result for limited motions of ions. Such mechanisms have been intensively discussed for many colloidal systems, including solutions of biopolymers as well as such of ionic micelles and vesicles. Fig. 2.16 shows the complex dielectric spectrum of an aqueous solution of a cationic surfactant with a conductivity contribution due to drift ions and with a solute relaxation term resulting from the limited motions of counterions on the surface of micelles. As a result of Coulombic interactions most counterions are condensed on the micellar surface where they form a diffusive layer around the micellar aggregate.

Relaxation terms with large amplitudes and relaxation times result if the limited motions extend over distances larger than molecular dimensions [12]. Such a "giant" dispersion is shown in Fig. 2.17 for an aqueous suspension of erythrocytes. Notice that in this diagram ε' and ε'' are displayed on a logarithmic scale.

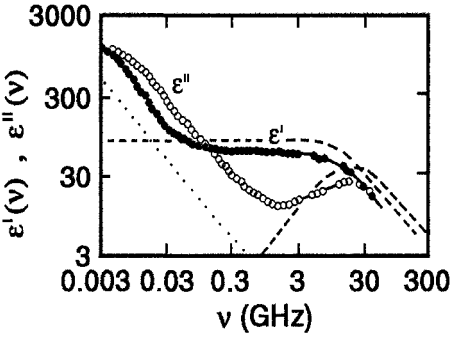

Fig. 2.17. Bilogarithmic plot of the permittivity spectrum of a solution of erythrocytes [9]. Again the dotted line represents the conductivity contribution and the dashed curves indicate the water spectrum at 25°C

Solute contributions with relaxation characteristics result also from incomplete dissociation of multivalent salts which, in many cases, is described by the Eigen-Tamm scheme [13]

$$(M^{m+})_{aq} + (A^{a-})_{aq} \Leftrightarrow (M^{m+}(H_2O)_2 A^{a-})_{aq}$$
$$(M^{m+}(H_2O)A^{a-})_{aq} \Leftrightarrow (MA)^{m-a}_{aq} \qquad (2.14)$$

where M^{m+} is a metal cation and A^{a-} an anion. The $(M^{m+}(H_2O)_2A^{a-})_{aq}$ complex with the anion separated from the cation by two layers of water molecules is called an "outer-outer-sphere" complex or "Bjerrum ion pair". The species $(M^{m+}(H_2O)A^{a-})_{aq}$ is called an "outer sphere" complex, and $(MA)^{m-a}$ the contact ion pair.

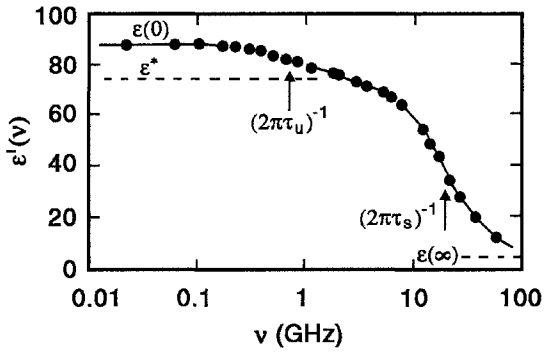

Fig. 2.18. Real part of the dielectric spectrum of a 0.1 molar aqueous solution of $Sc_2(S0_4)_3$ at 25°C [6]

The dielectric relaxation process and the effects in the ionic conductivity of the solutions which result from the complex formation are well established. An example of the real part of the permittivity spectrum for a solution of a 3:2 valent electrolyte is shown in Fig. 2.18. As another example the dielectric spectrum of a solution of 3:2 valent aluminum sulfate is compared to that of aluminum chloride in Fig. 2.19. A suggestive complex plane representation of data is given, in which the negative imaginary part of the spectrum, excluding conductivity contributions, is plotted versus the real part. For water, for which the spectrum can be well represented by a Debye type relaxation (Eq. (2.5)), the data define a semicircle with its center on the ε' axis. A semicircle with center somewhat below the ε' axis follows for the solution of 3:1 valent aluminium chloride, indicating a small distribution of relaxation times due to the disturbance of the water properties by the solute. The spectrum for the aluminium sulfate solution clearly displays two relaxation regions, of which the low frequency one reflects the reorientational motions of the dipolar ion pairs (Eq. (2.14) with $M^{m+} = Al^{3+}$ and $A^{a-} = SO_4^{2-}$). Two and three valent transition metal ions with d^{10} outer electron shell are able to form dielectrically evident ion complex structures even with monovalent ligands like the halides.

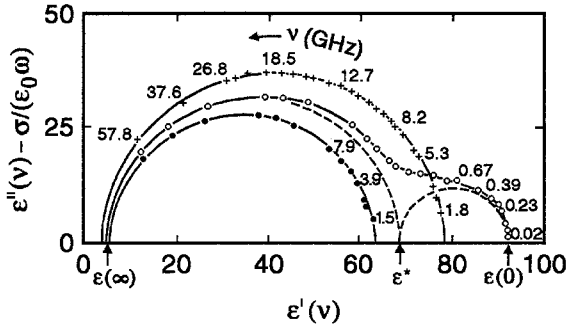

Fig. 2.19. Complex plane representation of the permittivity spectra excluding conductivity contributions for water (+), and aqueous solutions of $AlCl_3$ (0.4 mol/l, •) and of $Al_2(SO_4)_3$ (0.15 mol/l, O) at 25°C. Dashed lines show the subdivision of the latter into a solvent and a solute contribution

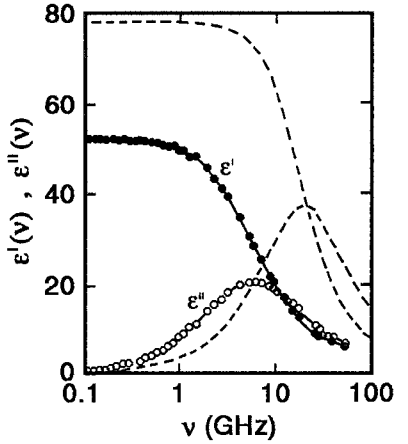

Fig. 2.20. Complex dielectric spectra for water (dashed curves) and for a 4.4 mol/l solution of *tert*-butanol in water at 25°C[9]

Many mixtures of water with dipolar solutes do not show well separated solute and solvent dielectric relaxation regions like the aqueous solutions of 4-aminobutyric acid (Fig. 2.15). Rather the spectra reflect a dielectrically homogeneous mixture with one principal relaxation, subject to a relaxation time distribution as represented, for instance, by the Havriliak–Negami spectral function (Eqs. (2.11, 2.12)). Examples are mixtures of water with alcohols, alkanediols, mono- and disaccharides, urea and its derivatives, dimethylsulfoxide, and various others. In Fig. 2.20, the real part ε' and the negative imaginary part ε'' of the complex permittivity are displayed as a function of frequency ν for a mixture of tert-butanol with water to illustrate the existence of essentially one dispersion region only. Fig. 2.21 presents a complex plane representation for the permittivity spectrum of an aqueous solution of D-glucose. This diagram shows the strong deformation of the original circular arc plot for water. With the saccharide solution there exists a broad relaxation time distribution due to the different reorientational motions of the D-glucose molecules, their dipolar side groups, as well as of the water molecules. The latter will display a relaxation time distribution by themselves because they are differently affected by the solute.

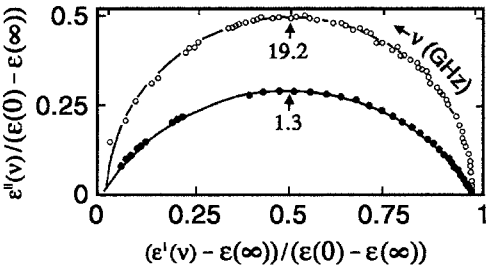

Fig. 2.21. Complex plane representation of the dielectric spectra for water (○) and for an aqueous solution of D-glucose (4.73 mol/l, •) at 25°C

2.5.2 Solvent Permittivity Contribution Aspects

The extrapolated low frequency permittivity ε^* of the water contribution to the dielectric spectra (Figs. 2.18, 2.19) offers valuable information on structural properties of the liquid. For solutions of nondipolar solutes $\varepsilon^* = \varepsilon(0)$. First of all, however, ε^* reflects the effect of dilution of the dipolar solvent, namely the reduction of the concentration c in Eq. (2.7) by the presence of the solute. Due to internal electric fields in dielectric mixtures ε^* depends also on the shape of the solute particles. This effect is sometimes used as a tool to investigate structural aspects of dielectrically heterogeneous systems like micro-emulsions. Unfortunately, however, even for homogeneous solutions of spherically shaped solute particles the effect of internal fields cannot be rigorously considered. Different theoretical approaches have lead to a multitude of mixture relations relating the resulting permittivity ε_2 of solutions of spherical solutes with permittivity ε^* in a suspending medium with permittivity ε_1 to the properties of the constituents. The graphs of two prominent mixture relations [6, 7, 9] which are frequently applied to aqueous systems are displayed in Fig. 2.22. Shown for aqueous solutions at 25°C ($\varepsilon_1 = \varepsilon(0) = 78.36$, Table 2.1; $\varepsilon_2 = 2$) are the Bruggeman formula

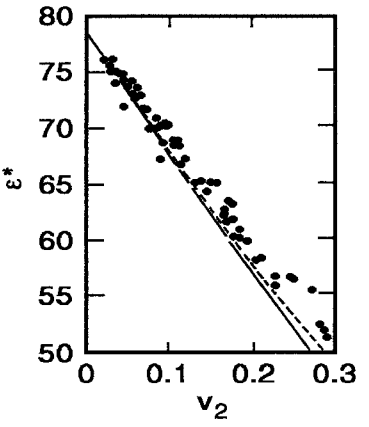

Fig. 2.22. Solvent contribution ε^* to the static permittivity versus volume fraction v_2 of solute for aqueous solutions of small organic molecules, of synthetic polymers, and of salts with large organic cations at 25°C [6, 7]. The line is the graph of the Bruggeman relation (Eq. (2.15))

$$\frac{\varepsilon^* - \varepsilon_2}{\varepsilon_1 - \varepsilon_2}\left(\frac{\varepsilon_1}{\varepsilon^*}\right)^{1/3} = 1 - v_2 \tag{2.15}$$

and a mixture relation originally derived by Maxwell and Wagner:

$$\varepsilon^* = \varepsilon_1 + \frac{3v_2(\varepsilon_2 - \varepsilon_1)}{2\varepsilon_1 + \varepsilon_2 - v_2(\varepsilon_2 - \varepsilon_1)} \tag{2.16}$$

In these formulas v_2 denotes the volume fraction of solute.

Also given in Fig. 2.22 for comparison are ε^* data for aqueous solutions of organic solutes. Interestingly, the scatter in the ε^* data for different series of solutes is comparatively small, thus indicating that the static permittivitiy of water depends only weakly on the particular interactions with the solute. The tendency in the experimental data to somewhat exceed the predictions from the mixture relations (Eqs. (2.15), (2.16)) seems to be characteristic to so-called "hydrophobic hydration" effects around largely inert molecules or ions. On the contrary, around small inorganic ions the effects from the above mentioned dielectric saturation may result in a substantial reduction of the extrapolated permittivity ε^* (Fig. 2.23). Besides the preferential orientation of water dipole moments in strong Coulombic fields, the extrapolated low frequency permittivity of electrolyte solutions may be also subject to a kinetic polarization deficiency [6, 7]. The model of kinetic depolarization proceeds from the idea that a charged particle moving through a dipolar liquid in an external electric field sets up a non-uniform hydrodynamic flow. The solvent dipole moments are turned by this flow in the direction opposed to that in which they are oriented by the electric field.

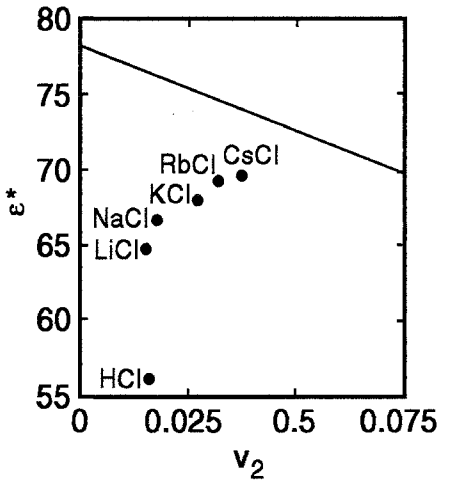

Fig. 2.23. Solvent contribution ε^* (= $\varepsilon(0)$) to the extrapolated low frequency permittivity for 1 mol/l solutions of some monovalent chlorides in water at 25°C [7]. The line is the graph of the mixture formula defined by Eq. (2.15)

It is common practice to express the effect of the solute on the principal dielectric relaxation time τ_s of the relative molal shift

$$B_d = \frac{1}{\tau_w} \lim_{m \to 0} \left(\frac{d\tau_s}{dm} \right) \tag{2.17}$$

and to assume the B_d values of electrolyte solutions to be simply given by the sum

$$B_d = \frac{m^+}{m} B_d^+ + \frac{m^-}{m} B_d^- \tag{2.18}$$

Here, B_d^+ and B_d^- denote the cationic and anionic relative molal shift and m, m^+ as well as m^- are the molal concentrations of electrolyte, cations, and anions, respectively. In Table 2.2 B_d and B_d^+ data for some series of organic molecules and ions are given. Within each series the tendency emerges for the relative shift in the relaxation time to increase with the number of aliphatic groups per solute particle. This tendency is a reflection of the aforementioned hydrophobic hydration. Within the framework of the above wait-and-switch model of dielectric relaxation the increase in the dielectric relaxation time of water around hydrophobic molecules or groups results mainly from the reduced density of hydrogen bonding sites and thus of suitable additional neighbor molecules at the water-solute interface. However, factors other than the local availability of additional hydrogen bonding partners are also important in determining the water relaxation time. These factors may include the overall size and shape of solute molecules, its flexibility with respect to the water structure, and the steric arrangement of its hydrophilic groups. Examples are the B_d–values for the stereoisomers N,N'- dimethylurea (B_d= 0.18(mol/kg)$^{-1}$) and ethylurea (B_d= 0.13(mol/kg)$^{-1}$).

An opposite effect, namely a reduction of the relaxation time τ_s with respect to τ_w is also found ($B_d < 0$). The ammonium ion shows indications of weak "negative hydration". A prominent example of the effects of negative hydration is the iodide ion with B_d^+ = -0.05 (mol/kg)$^{-1}$. Around this large monovalent anion an enhanced mobility of water molecules may result from the comparatively soft electron shell, providing reorientating water molecules with transient hydrogen bond-like interactions. Hence, at least in parts, negative hydration may be also discussed in terms of the wait-and-switch model. A more detailed discussion of the dielectric properties of aqueous solutions is given in a more recent review article [7] where complex permittivity spectra are also considered in the light of a hydration model.

Table 2.2. Relative molar shifts B_d as well as cationic part B_d^+ in the principal relaxation time τ_s of water for aqueous solutions of some series of molecules and organic ions (25°C, pyridine and derivatives 20°C [6]).

Solute	B_d (mol/kg)$^{-1}$	Solute	B_d (mol/kg)$^{-1}$
Pyrazine	0.13	Urea	0.03
Methylpyrazine	0.19	Methylurea	0.08
2,3-Dimethylpyrazine	0.24	N,N-Dimethylurea	0.17
2,5-Dimethylpyrazine	0.27	N,N'-Dimethylurea	0.18
2,6-Dimethylpyrazine	0.25	Ethylurea	0.13
Ethylpyrazine	0.21	Trimethylurea	0.24
2,3,5-Trimethypyrazine	0.32	N-Propylurea	0.19
Quinoxaline	0.19	Tetramethylurea	0.30
2-Methylquinoxaline	0.24	N,N-Diethylurea	0,30
Pyridine	0.19	N-Butylurea	0.21
2-Methylpyridine	0.27		
3-Methylpyridine	0.22		
2,4-Diemthylpyridine	0.27		
2,6- Diemthylpyridine	0.28		
Cation	B_d^+ (mol/kg)$^{-1}$	Cation	B_d^+ (mol/kg)$^{-1}$
Ammonium	-0.04	Tetramethylammonium	0.17
N-Butylammonium	0.28	Tetraethylammonium	0.39
N-Hexylammonium	0.37	Tetrapropylammonium	0.73
N-Heptylammonium	0.38	Tetrabutylammonium	0.88
N-Octylammonium	0.44	5-Azoniaspiro[4,4]nonane	0.29
		6-Azoniaspiro[5,5]undecane	0.37
		7-Azoniaspiro[6,6]tridecane	0.43

2.6 Conclusions: Microwave Aquametry, an Inverse Problem

In microwave aquametry, we are normally dealing with a sophisticated inverse problem. We measure over a more or less broad frequency range the resulting permittivity $\varepsilon(\nu)$ of a composite dielectric and we want to calculate from it the volume fraction $v_1 = 1 - v_2$ of one of the constituents, namely the water. This is an intricate attempt, because $\varepsilon(\nu)$ does not just depend on v_l but also on shape characteristics of the dielectric mixture and on the permittivities ε_1 and ε_2 of the aqueous and the non-aqueous phase. The evaluation of the experimental data is more difficult as, because of the internal polarising and depolarising electric fields, the permittivity of mixtures cannot be calculated rigorously. Hence, as already mentioned above, many different mixture relations exist even for solutions of simply shaped spherical and ellipsoidal solutes, each formula reflecting the particular assumptions made in the theoretical treatment of the problem. Irrespective of the

theoretical model, the determination of the desired volume fraction v_l from the mixture permittivity $\varepsilon(\nu)$ requires also the most accurate knowledge of the dielectric properties of the constituents. Much progress has been made in the past decades in our understanding of the complex permittivity behavior of water as a function of frequency, temperature, and hydrostatic pressure. There exists also a large amount of data characterizing the dielectric properties of aqueous solutions, which is important since the aqueous constituent in microwave aquametry often will not just be water. In this short tutorial only some effects of solutes on the features of water have been presented and considered in the light of recent ideas about dielectric relaxation of hydrogen bonding dipolar liquids. Attention has been also directed toward solute contributions which, on various events, may dominate the complex permittivity of aqueous solutions.

References

1. Franks F (1972) Introduction – Water, the unique chemical. In: Franks F (ed) Water, a comprehensive treatise, vol 1. Plenum, New York, pp 1–20
2. Kaatze U (1989) Complex permittivity of water as a function of frequency and temperature. J. Chem. Eng. Data 34: 371–374
3. Ellison WJ, Lamkaouchi K, Moreau JM (1996) Water: a dielectric reference. J. Molec. Liquids 68: 171–279
4. Kaatze U (1996) Microwave dielectric properties of water. In: Kraszewski A (ed) Microwave aquametry. Electromagnetic wave interactions with water-containing materials. IEEE Press, New York, pp 37–53
5. Kaatze U (2000) Hydrogen network fluctuations and the microwave dielectric properties of liquid water. Subsurface Sensing Technol. Applic. 4: 377–391
6. Kaatze U (1995) Microw. dielec. properties of liquids. Rad. Phys. Chem. 45: 549–566
7. Kaatze U (1997) The dielectric properties of water in its different states of interaction. J. Solution Chem. 26: 1049–1112
8. Barthel JMG, Krienke H, Kunz W (1998) Physical chemistry of electrolyte solutions. Modern aspects. Steinkopff, Darmstadt
9. Kaatze U, Behrends R (2002) Dielektrische Eigenschaften von Wasser und wässrigen Lösungen. Technisches Messen 69: 5–11
10. Kaatze U, Behrends R, Pottel R (2002) Hydrogen network fluctuations and dielectric spectrometry of liquids. J. Non-Crystalline Solids 305: 19–28
11. Pottel R, Asselborn E, Eck R, Tresp V (1989) Dielectric relaxation rate and static dielectric permittivity of water and aqueous solutions at high pressures. Ber. Bunsenges. Phys. Chem. 93: 676–681.
12. Dukhin SS, Shilov VN (1974) Dielectric phenomena and the double layer in disperse systems and polyelectrolytes. Halsted, New York
13. Pottel R (1966) The complex dielectric constant of some aqueous electrolyte solutions in a wide frequency range. In: Conway BE, Barradas RG (eds) Chemical physics of ionic solutions. Wiley, New York
14. Marsh KN (1981) I.U.P.A.C. Recommended reference materials. Permittivity. Pure Appl. Chem. 53: 1847–1862